Spectral tuning of plasmon-enhanced silicon quantum dot luminescence

Julie S. Biteen,[a] Nathan S. Lewis, and Harry A. Atwater
California Institute of Technology, 1200 East California Boulevard, Pasadena, California 91125

Hans Mertens and Albert Polman
Center for Nanophotonics, FOM Institute for Atomic and Molecular Physics, Kruislaan 407,
1098 SJ Amsterdam, The Netherlands

In the presence of nanoscale silver island arrays, silicon quantum dots exhibit up to sevenfold luminescence enhancements at emission frequencies that correspond to the collective dipole plasmon resonance frequency of the Ag island array. Using electron-beam lithography to alter the pitch and particle diameter, this wavelength-selective enhancement can be varied as the metal array resonance wavelength is tuned from 600 to 900 nm. The luminescence intensity enhancement upon coupling is attributed to an increase in the radiative decay rate of the silicon quantum dots. © *2006 American Institute of Physics*. [DOI: 10.1063/1.2191411]

Since the observation in 1990 of strong room-temperature photoluminescence from porous silicon,[1,2] significant worldwide interest has been directed toward silicon-based photonics for integrated optoelectronics. An integral part of such systems is a Si-based, power-efficient light emitter. From that perspective, silicon quantum dots (Si QDs) have been intensively investigated as light sources. Si QDs exhibit efficient room-temperature luminescence due to the radiative recombination of quantum-confined excitons, and their emission frequency can be tuned through part of the visible and near-infrared spectrum by varying the QD size[3] or surface termination.[4] However, Si QDs suffer from low radiative decay rates relative to those of direct band gap semiconductors and organic dyes. Coupling of radiative dipole emission to metal nanostructures provides an opportunity to enhance the Si QD radiative decay rate, as previous reports have shown for semiconductor QDs (Refs. 5–7) and quantum wells.[8] Enhanced radiative emission has been attributed to electromagnetic coupling between the semiconductor active dipole emitters and surface plasmons in the metal. This coupling, which is stronger at frequencies near the plasmon resonance, can result in enhancements of the emission intensity and of the decay rates.[9]

In this letter, we report an enhancement of photoluminescence (PL) in Si QDs coupled to Ag island arrays fabricated by electron-beam lithography. When the surface plasmon resonance of the Ag island arrays is tuned throughout the Si QD emission spectrum, we observe a strong correlation between the frequency at which the PL emission is enhanced and the surface plasmon resonance frequency. From this behavior, we conclude that the observed PL enhancement is caused by an enhancement of the radiative decay rate of the Si QDs.

Si QDs were produced by ion implantation of 11-keV Si^+ ions to a fluence of 1.7×10^{16} cm^{-2} into a 1.6-mm-thick fused quartz strip (Technical Glass Products). Monte Carlo simulations performed with SRIM (Ref. 10) indicate that such an implantation yields a Gaussian depth distribution of Si in the SiO_2, with a peak excess Si concentration of 10% at a depth of ~20 nm. The implanted quartz was annealed in Ar for 20 min each at 200 and 450 °C, and then for 30 min at 1000 °C, to form Si QDs with typical diameters of 3–5 nm.[11] The samples were subsequently heated in forming gas (10% H_2, 90% N_2) for 30 min at 450 °C to eliminate emission from defect states in the SiO_2 matrix.[12] After Si QD formation, the QD distribution was brought to an average depth Δ of 8, 13, or 18 nm from the surface by etching in 2.3% HF(aq). The etch rate was 0.25 nm/s, as determined by spectroscopic ellipsometry (Sentech SE-850) on an analogous sample of SiO_2 on a Si substrate. Ellipsometry also indicated that after etching, the surface roughness was less than ±0.2 nm.

To obtain the strongest possible plasmonic effects, the Si-QD-doped SiO_2 was coupled to Ag nanoparticles. Silver was chosen because it has the lowest absorption and produces the strongest resonances among all metals with plasmon resonances at visible frequencies. The surface of the QD-doped quartz was cleaned in a 5:1:1 $H_2O:H_2O_2:NH_4OH$ solution. An electron beam was used to pattern 100 μm × 100 μm arrays of circles on two layers of polymethylmethacrylate (PMMA) covered by a 17 nm Ge conduction layer. After removing the Ge and developing the resist, a 2 nm Si wetting layer and a 20 nm Ag layer were deposited onto the structure by electron-beam evaporation under ultrahigh vacuum conditions. The remaining PMMA was lifted off, leaving arrays of cylindrical Ag islands. The resulting structure is sketched in Fig. 1(a), and scanning electron micrograph (SEM) images of one series of Ag arrays, with a 400 nm pitch and increasing diameters (135–390 nm), are displayed in Fig. 1(b).

Each array of Ag islands with height $h = 20$ nm was characterized by a distinct pitch p (200–500 nm), particle diameter d (100–440 nm), and thus cylinder aspect ratio $a = d/h$ (5–22). As a consequence of these geometric differences, the arrays were characterized by distinct plasmon resonance frequencies,[13] which were determined by measuring the transmission spectrum through each Ag island array. For the transmission measurement, the arrays were illuminated with a white light source incident through a 60× microscope objective, and the transmitted light was collected with a 20× microscope objective. The spectral transmittance through each Ag island array was normalized by the transmittance through a nearby region devoid of Ag islands.

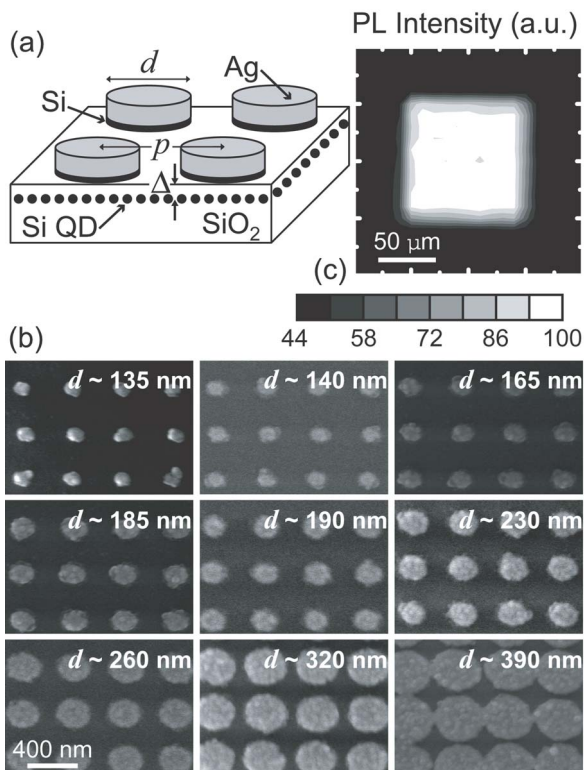[a]Author to whom correspondence should be addressed; electronic mail: jsbiteen@caltech.edu

FIG. 1. (a) Array of Ag nanoparticles with diameter d and pitch p on Si-QD-doped quartz. (b) SEM images of a series of Ag nanoparticle arrays with $p=400$ nm and $d=135–390$ nm. (c) PL intensity map over a representative Ag array ($p=400$ nm, $d=320$ nm, and $\Delta=8$ nm) in 10-μm steps, integrated from $\lambda=640$ to 950 nm.
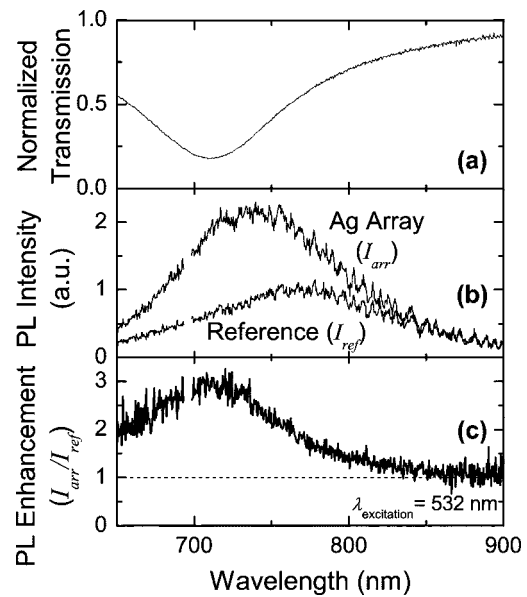

FIG. 2. Optical characterization of a representative sample ($p=400$ nm, $d=320$ nm, and $\Delta=13$ nm). (a) Normalized transmission through the Ag nanoparticle array. (b) PL intensity from Si QDs in the absence (bottom curve) and presence (top curve) of Ag islands. (c) PL intensity enhancement [ratio of curves in (b)].

PL spectra were acquired under excitation from a frequency-doubled Nd:YAG (yttrium aluminum garnet) laser operating at $\lambda_{\text{excitation}}=532$ nm focused through a microscope objective to a 10-μm-diam spot. A relatively high pump power, 10^4 W/cm^2, was used to ensure operation near the saturated pump power regime, where the PL emission is limited by the radiative decay rate and is independent of the quantum efficiency. The PL intensity was recorded using a thermoelectrically cooled charge-coupled device detector (sensitivity range of 200–1100 nm) in conjunction with a 30 cm focal length grating spectrograph. A dichroic filter that absorbs wavelengths below 550 nm was used to eliminate incident laser light from the detector. Si QD excitation and PL emission collection were performed both through the Ag arrays and through the quartz substrate, and all of these combinations gave similar results for the enhancement magnitude and spectral dependence, indicating that the Si/Ag system was acting as a coupled entity. Reference luminescence measurements were obtained from a region of Si-QD-doped quartz not located under a Ag island array. To check for PL signal uniformity over the range of the 100 μm $\times$ 100 μm particle arrays, as well as over the range of the Ag-free reference areas, the samples were mounted on a translation stage and the PL intensity was measured in 10-μm steps. Figure 1(c) shows a typical result for such a two-dimensional scan ($d=320$ nm, $p=400$ nm, and $\Delta=8$ nm). The PL intensity (integrated from $\lambda=640$ to 950 nm) emitted from the array region was approximately twice that emitted from the uncoupled QDs in the reference areas, and the PL intensity was essentially constant in both areas. The spatial resolution of this measurement is not sufficient to identify differences

in PL intensity at length scales smaller than the pitch.

Figure 2 shows the correspondence between the spectral position and shape of the Si QD PL enhancement and the surface plasmon resonance of a typical Ag island array/Si QD system ($d=190$ nm, $p=400$ nm, and $\Delta=13$ nm). The normalized transmission spectrum of the array [Fig. 2(a)] exhibited a dip centered at 710 nm that can be attributed to extinction due to the excitation of dipole plasmon modes in the Ag islands. As illustrated in Fig. 2(b), the PL intensity on the array I_{arr} was enhanced significantly compared to the Si QD PL intensity in the reference area I_{ref}, especially at wavelengths where the plasmon mode is resonant. Figure 2(c) shows the PL enhancement spectrum, $I_{\text{arr}}(\lambda)/I_{\text{ref}}(\lambda)$. The enhancement spectrum corresponds strongly with the transmission spectrum, peaking at $\lambda=710$ nm.

Figure 3 shows normalized transmission and PL enhancement spectra for six samples with Ag island arrays that have an increasing island diameter from top to bottom at a fixed 400 nm pitch and $\Delta=13$ nm. As d was increased, the transmission dip grew larger in magnitude and shifted to larger wavelengths. The decreased transmission is attributable to an increase in Ag coverage. The shift of the minimum transmission wavelength can be understood qualitatively based on the increase in d (from 665 to 320 nm) and in a (from 8 to 16), which are both known to cause a redshift of the surface plasmon resonance in the plane of these arrays.[13]

The PL enhancement spectra (Fig. 3) exhibited a redshift with increasing d and a that is similar to the trend in transmission dips, establishing a strong correlation between the PL enhancement and the surface plasmon resonance. This correspondence is illustrated for 187 different samples in Fig. 4(a), in which the wavelength of minimum transmission is correlated with the maximum PL enhancement wavelength. The observed trend is well fitted by a straight line with a slope of 0.97 ± 0.03 and a y intercept of 14 ± 17 nm. Despite variations in Δ, p, and d, the strong spectral correspondence between Si QD PL enhancement and particle ar-
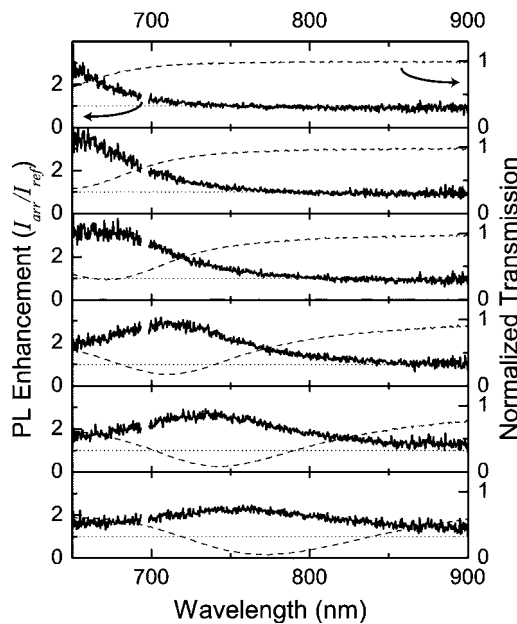
FIG. 3. PL intensity enhancement (solid lines) and normalized transmission spectra (dashed lines) for samples with $p=400$ nm and $\Delta=13$ nm; d increases from the top to bottom panels, with $d=165$, 185, 190, 230, 260, and 320 nm, respectively.

ray plasmon resonance indicates that the PL enhancement can consistently be ascribed to an increase in radiative decay rate due to resonant coupling of the Si QDs with collective surface plasmon modes of the Ag islands. No luminescence enhancements were observed for samples that show transmission dips resonant with the 532 nm excitation source, demonstrating that the increased PL intensity cannot be attributed to increased pump power absorption.

Figure 4(b) shows the magnitude of the maximum PL intensity enhancement as a function of wavelength for 201 different samples. Coupling Si QDs to Ag island arrays produces up to sevenfold enhancements, and the greatest increases are observed at short emission wavelengths, where smaller nanoparticles are resonant. It is expected that only Si

QDs positioned closer to Ag particles than the typical plasmon coupling range of ~ 50 nm experience an enhanced emission rate.[9] It follows that the number of Si QDs coupled to Ag islands increases with particle coverage. The fact that a smaller overall PL enhancement is found for larger particles thus implies that the emission enhancement per QD must be greater near the smaller particles. This behavior is consistent with trends in radiative damping of the excited plasmon mode and in local field enhancement as a function of particle size; the former, which limits the radiative decay rate enhancement, is more significant for larger nanoparticles,[14] while the local field enhancement about metal particles decreases with increasing size.[15] The samples considered in Fig. 4 have $d=100-440$ nm, $p=200-500$ nm, and $\Delta =8-18$ nm, yet the magnitude of enhancement was found to depend most strongly on d. This indicates that the pitch has a more subtle influence, and that effects due to the Si–Ag separation distances were likely obfuscated by the large spread in Si QD depths about the average depth Δ.

In conclusion, we have observed up to sevenfold enhancements in PL intensity of Si QDs upon coupling to Ag island arrays. The enhancement can be spectrally controlled between 600 and 900 nm by tuning the surface plasmon resonance frequency of the Ag islands through varying the island diameter and the array pitch. Coupling to engineered plasmonic structures thus provides an interesting approach to controlling the emission rate and emission spectrum of Si quantum dots.
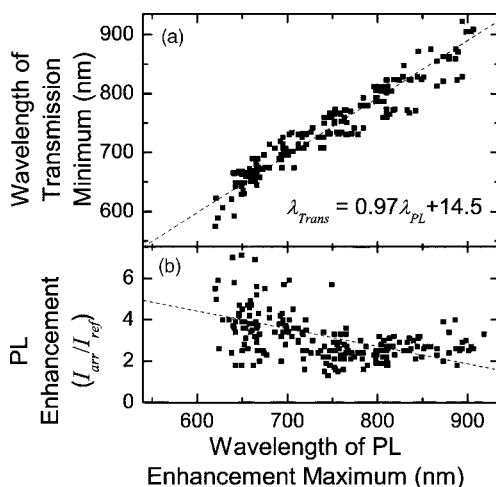
FIG. 4. (a) Correspondence between the wavelength of minimum transmission and the wavelength of maximum PL enhancement for 187 different samples. (b) Comparison between the maximum magnitude of PL enhancement and the wavelength at which this maximum is reached for 201 different samples.

[1] L. T. Canham, Appl. Phys. Lett. **57**, 1046 (1990).
[2] A. G. Cullis and L. T. Canham, Nature (London) **353**, 335 (1991).
[3] T. Fischer, V. Petrova-Koch, K. Shcheglov, M. S. Brandt, and F. Koch, Thin Solid Films **276**, 100 (1996).
[4] M. V. Wolkin, J. Jorne, P. M. Fauchet, G. Allan, and C. Delerue, Phys. Rev. Lett. **82**, 197 (1999).
[5] O. Kulakovich, N. Strekal, A. Yaroshevich, S. Maskevich, S. Gaponenko, I. Nabiev, U. Woggon, and M. Artemyev, Nano Lett. **2**, 1449 (2002).
[6] K. T. Shimizu, W. K. Woo, B. R. Fisher, H. J. Eisler, and M. G. Bawendi, Phys. Rev. Lett. **89**, 117401 (2002).
[7] J. S. Biteen, D. Pacifici, N. S. Lewis, and H. A. Atwater, Nano Lett. **5**, 1768 (2005).
[8] K. Okamoto, I. Niki, A. Shvartser, Y. Narukawa, T. Mukai, and A. Scherer, Nat. Mater. **3**, 601 (2004).
[9] J. Gersten and A. Nitzan, J. Chem. Phys. **75**, 1139 (1981).
[10] J. F. Ziegler, J. P. Biersack, and U. Littmark, *The Stopping and Range of Ions in Solids* (Pergamon, New York, 1985).
[11] K. S. Min, K. V. Shcheglov, C. M. Yang, H. A. Atwater, M. L. Brongersma, and A. Polman, Appl. Phys. Lett. **69**, 2033 (1996).
[12] K. S. Min, K. V. Shcheglov, C. M. Yang, H. A. Atwater, M. L. Brongersma, and A. Polman, Appl. Phys. Lett. **68**, 2511 (1996).
[13] Craig F. Bohren and Donald R. Huffman, *Absorption and Scattering of Light by Small Particles* (Wiley, New York, 1983).
[14] A. Wokaun, J. P. Gordon, and P. F. Liao, Phys. Rev. Lett. **48**, 957 (1982).
[15] K. L. Kelly, E. Coronado, L. L. Zhao, and G. C. Schatz, J. Phys. Chem. B **107**, 668 (2003).